Monthly Notices
of the
ROYAL ASTRONOMICAL SOCIETY

MNRAS **483,** 4031–4039 (2019)
Advance Access publication 2018 December 11

doi:10.1093/mnras/sty3357

# The suppression of star formation on the smallest scales: what role does environment play?

M. K. Rodriguez Wimberly [1]★ M. C. Cooper [1] S. P. Fillingham [1]
M. Boylan-Kolchin [2] J. S. Bullock [1] and S. Garrison-Kimmel [3]†

[1] *Center for Cosmology, Department of Physics & Astronomy, 4129 Reines Hall, University of California, Irvine, CA 92697, USA*
[2] *Department of Astronomy, The University of Texas at Austin, 2515 Speedway, Stop C1400, Austin, TX 78712, USA*
[3] *TAPIR, Mailcode 350-17, California Institute of Technology, Pasadena, CA 91125, USA*

Accepted 2018 December 5. Received 2018 December 4; in original form 2018 June 19

## ABSTRACT

The predominantly ancient stellar populations observed in the lowest mass galaxies (i.e. ultra-faint dwarfs) suggest that their star formation was suppressed by reionization. Most of the well-studied ultra-faint dwarfs, however, are within the central half of the Milky Way dark matter halo, such that they are consistent with a population that was accreted at early times and thus potentially quenched via environmental processes. To study the potential role of environment in suppressing star formation on the smallest scales, we utilize the Exploring the Local Volume in Simulations suite of *N*-body simulations to constrain the distribution of infall times for low-mass subhaloes likely to host the ultra-faint population. For the ultra-faint satellites of the Milky Way with star formation histories inferred from *Hubble Space Telescope* imaging, we find that environment is highly unlikely to play a dominant role in quenching their star formation. Even when including the potential effects of pre-processing, there is a $\lesssim$0.1 per cent probability that environmental processes quenched all of the known ultra-faint dwarfs early enough to explain their observed star formation histories. Instead, we argue for a mass floor in the effectiveness of satellite quenching at roughly $M_\star \sim 10^5\,\mathrm{M}_\odot$, below which star formation in surviving galaxies is globally suppressed by reionization. We predict a large population of quenched ultra-faint dwarfs in the Local Field ($1 < R/R_{\rm vir} < 2$), with as many as ∼250 to be discovered by future wide-field imaging surveys.

**Key words:** galaxies: dwarf – galaxies: evolution – galaxies: formation – galaxies: general – Local Group – galaxies: star formation.

## 1 INTRODUCTION

The Local Group serves as a cosmic Rosetta Stone, offering the opportunity to study galaxy formation and evolution at a level of detail not possible at cosmological distances (Boylan-Kolchin et al. 2016). This is especially true at the smallest galactic scales – i.e. for very low-mass galaxies or what are often referred to as ultra-faint dwarfs (UFDs). Photometric observations of UFDs in the Local Group find universally old stellar populations, such that these systems have typically ceased forming stars by $z \sim 2$ (or a lookback time of ∼10.3 Gyr, Brown et al. 2014; Weisz et al. 2014b). The prevalence of ancient stellar components in these extremely low-mass systems is commonly interpreted as evidence of star formation suppression via reionization, where a photoionizing background increases the cooling time for low-density gas so as to quell the fuel supply for star formation in the lowest mass haloes (e.g. Efstathiou 1992; Quinn, Katz & Efstathiou 1996; Thoul & Weinberg 1996).

While the measured star formation histories (SFHs) of UFDs are broadly compatible with quenching via reionization, the most well-studied systems in the Local Group are located at relatively small galactocentric radii, which is also consistent with a population that was accreted at early cosmic time (Rocha, Peter & Bullock 2012; Oman, Hudson & Behroozi 2013). As such, the old stellar populations identified in UFDs orbiting the Milky Way and M31 may instead be the result of environmental processes that quenched star formation following infall on to the host halo. For example, recent measurements of the proper motion for the Segue I dwarf (Belokurov et al. 2007) suggest that it was accreted by the Milky Way halo roughly 9.4 Gyr ago (Fritz et al. 2018a), such that rapid environmental quenching would produce an ancient and metal-poor stellar population as observed today (Frebel, Simon & Kirby 2014; Webster, Frebel & Bland-Hawthorn 2016). Undoubtedly,

★ E-mail: wimberlm@uci.edu
† Einstein fellow.

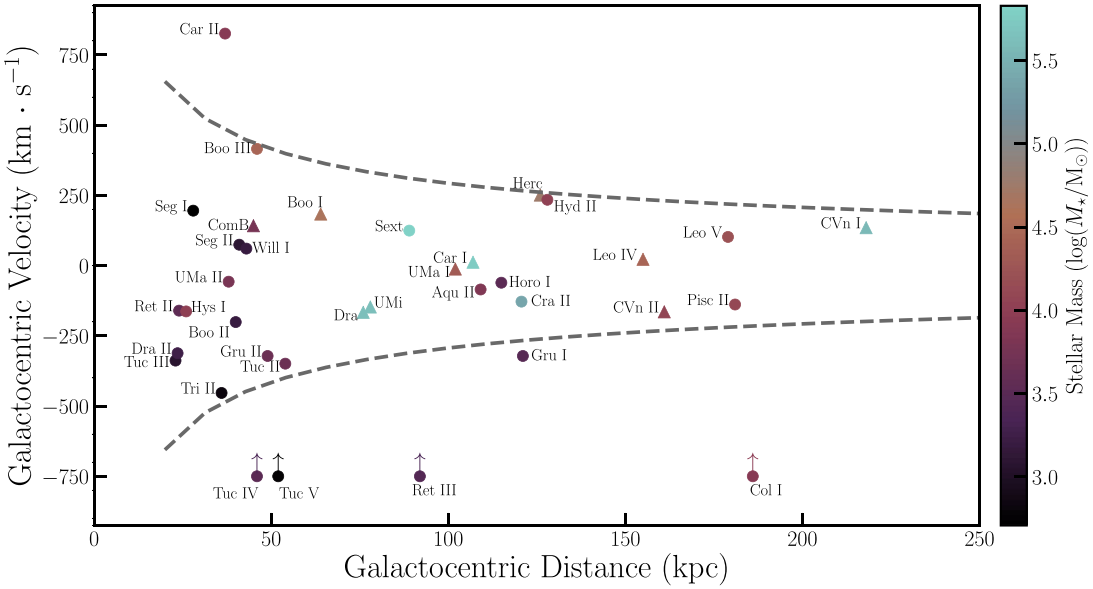


**Figure 1.** Galactocentric velocity versus distance for the sample of UFD satellites of the Milky Way. Points are colour-coded according to stellar mass, assuming a *V*-band mass-to-light ratio of 1.2; the triangles denote those objects with a published SFH from Brown et al. (2014) or Weisz et al. (2014b). To account for unknown tangential motion, the observed line-of-sight velocities have been multiplied by a factor of $\sqrt{3}$. Those systems without published line-of-sight velocity measurements (Tuc IV, Tuc V, Ret III, and Col I) are plotted at $\sqrt{3} \cdot V_{\ell os} = -750\,\mathrm{km\,s^{-1}}$ with upward arrows representing the uncertainty in their $V_{\ell os}$. Masses (i.e. luminosities), distances, and line-of-sight velocities for this sample are based on published values from McConnachie (2012), Bechtol et al. (2015), Drlica-Wagner et al. (2015), Laevens et al. (2015a), Brown et al. (2014), Weisz et al. (2014b), Simon et al. (2015, 2017), Kirby, Simon & Cohen (2015a), Kirby et al. (2013, 2015b, 2017), Li et al. (2018), Torrealba et al. (2016), Torrealba et al. (2018), Caldwell et al. (2017), Martin et al. (2016a); Laevens et al. (2015b), Walker et al. (2016), Koposov et al. (2018), and references therein.

observations of isolated UFDs (i.e. beyond the reach of environmental effects) would be an excellent way to differentiate between these two physical scenarios (quenching via reionization versus via environment). Current data sets, however, lack the depth to identify and characterize the stellar populations of UFDs in the Local Field.

To address the potential role of environment in quenching UFDs, we utilize a suite of *N*-body simulations to track the accretion and orbital history of the low-mass subhaloes that host the UFD satellite population. Our approach is similar to that utilized by Rocha et al. (2012, see also Weisz et al. 2015), with the clear distinction that we aim to study the UFD satellites as an ensemble and not on an object-by-object basis. For example, herein, we study the likelihood that the six galaxies in the UFD sample from Brown et al. (2014) were accreted at early cosmic times, such that environmental quenching could reproduce their observed SFHs. Overall, we strive to quantify the likelihood that environmental effects can explain the universal ancient stellar populations in the lowest mass galaxies. In Section 2, we provide a brief census of the UFD satellite population of the Milky Way along with a description of our simulation data set and our primary analysis methods. In Section 3, we present our results regarding the role of environment in quenching UFDs. Finally, we conclude with a brief discussion and summary of our work in Sections 4 and 5, respectively.

## 2 DATA

### 2.1 UFD galaxy sample

Since the discovery of the first UFDs using photometric data from the Sloan Digital Sky Survey (SDSS; York et al. 2000), a large number of UFDs have been identified as satellites of the Milky Way (e.g. Willman et al. 2005a,b; Zucker et al. 2006a,b; Belokurov et al. 2010; Bechtol et al. 2015; Drlica-Wagner et al. 2015). Deep imaging of M31 has likewise uncovered a population of UFDs orbiting M31, with similarly old stellar populations (e.g. Martin et al. 2009; Weisz et al. 2014b; Skillman et al. 2017). Throughout this work, we focus our analysis on the ultra-faint satellite population of the Milky Way, selecting all systems with $L_V < 5 \times 10^5\,\mathrm{L}_\odot$ ($M_V > -9.3$) as UFDs. Fig. 1 shows the position and line-of-sight velocity of these systems relative to the Milky Way, with velocities scaled by a factor of $\sqrt{3}$ to crudely account for potential tangential motion.[1]

Of the 36 known UFD satellites of the Milky Way, there are published SFHs in the literature for 10 based on *Hubble Space Telescope* (*HST*) imaging from Brown et al. (2014) and Weisz et al. (2014b). For all 10 of these systems, the reported mean stellar age is $> 9$ Gyr with 90 per cent of the stars forming by $z \sim 2$. For the small number of objects included in both the Brown et al. (2014) and Weisz et al. (2014b) samples, there is relatively good agreement between the measured SFHs. The exception is CVn II, for which Weisz et al. (2014b) find a tail of star formation extending to $z \sim 1$. The *HST*/WFPC2 imaging analysed by Weisz et al. (2014b), however, is shallower and covers a smaller area than the *HST*/ACS imaging utilized by Brown et al. (2014), such that greater photometric errors may be increasing the dispersion in the main-sequence turn-off population and thereby yielding a broader SFH. Altogether, observations of the known UFD population orbiting the Milky Way suggest that these very low-mass systems have old stellar populations, with little star-formation activity since $z \sim 1$–2

[1]This typically serves as a lower limit to the total velocity, with the recently measured motions for a subset of UFDs from *Gaia* Data Release 2 (Fritz et al. 2018b; Simon 2018), yielding higher total velocities than our $\sqrt{3}V_{\ell os}$ estimate.

(e.g. Okamoto et al. 2008, 2012; de Jong et al. 2008; Sand et al. 2009, 2010, 2012; Brown et al. 2012; Martin et al. 2015; Bettinelli et al. 2018).

### 2.2 *N*-Body cosmological simulations

To investigate the role environmental mechanisms play in the quenching of UFDs, we utilize the Exploring the Local Volume In Simulations (ELVIS) suite of 36 high-resolution, cosmological zoom-in simulations of Milky Way-like haloes (Garrison-Kimmel et al. 2014). Within the suite, 24 simulations are of isolated Milky Way-like haloes and 12 are of Milky Way- and M31-like pairs. Each simulation occurs within a high-resolution uncontaminated volume spanning 2−5 Mpc in size with a particle mass of $1.9 \times 10^5\,\mathrm{M}_\odot$ and a Plummer-equivalent force softening length of $\varepsilon = 141$ physical parsecs. Within the high-resolution volumes, the halo catalogues are complete down to $M_{\rm halo} > 2 \times 10^7\,\mathrm{M}_\odot$, $V_{\rm max} > 8\,\mathrm{km\,s^{-1}}$, $M_{\rm peak} > 6 \times 10^7\,\mathrm{M}_\odot$, and $V_{\rm peak} > 12\,\mathrm{km\,s^{-1}}$ – thus sufficient to track the evolution of haloes hosting Local Group dwarfs with stellar masses of $\sim 10^{3-5}\,\mathrm{M}_\odot$. ELVIS adopts a ΛCDM (Λ cold dark matter) cosmological model based on *Wilkinson Microwave Anisotropy Probe* 7-yr data (Komatsu et al. 2011; Larson et al. 2011) with the following parameters: $\sigma_8 = 0.801$, $\Omega_{\rm m} = 0.266$, $\Omega_\Lambda = 0.734$, $n_{\rm s} = 0.963$, and $h = 0.71$.

As a dark matter-only simulation suite, ELVIS fails to capture the impact of the host baryonic component on the subhalo population. In short, the inclusion of a disc potential can substantially alter the subhalo distribution inside of the host virial radius by tidally disrupting subhaloes (D'Onghia et al. 2010; Brooks et al. 2013; Brooks & Zolotov 2014; Garrison-Kimmel et al. 2017b; Sawala et al. 2017). This subhalo destruction preferentially occurs in objects with early infall times and/or more radial orbits. As such, the distribution of subhalo infall times for a dark matter-only simulation (such as ELVIS) will be biased towards earlier cosmic times, so as to overestimate the role of environmental mechanisms in quenching star formation at high $z$.

To account for the impact of the host baryonic component, following the work of Fillingham et al. (2018), we implement a correction to the ELVIS subhalo population that will broadly capture the tidal effects of the host. Based on figs 5 and A2 from Garrison-Kimmel et al. (2017b), we model the ratio of subhaloes in dark matter-only versus hydrodynamic simulations of Milky Way-like hosts as

$$N_{\rm DMO}/N_{\rm HYDRO} = 40\,\mathrm{e}^{-22\,d_{\rm peri}/\mathrm{kpc}}\ (\mathrm{for}\ d_{\rm peri} < 50\,\mathrm{kpc}),$$

where $N_{\rm DMO}$ is the number of subhaloes that survive to present-day in a dark matter-only simulation, $N_{\rm HYDRO}$ is the corresponding subhalo count for a hydrodynamic simulation, and $d_{\rm peri}$ is the host-centric distance at pericenter in kpc. This relationship between pericentric passage and the likelihood of subhalo disruption is supported by a larger number of dark matter-only simulations of Milky Way-like hosts, run with (and without) an evolving disc potential (Kelley et al. 2018).

To mimic the disruption of subhaloes in ELVIS, we adopt $(N_{\rm DMO}/N_{\rm HYDRO})^{-1}$ as the likelihood that a subhalo survives to $z = 0$ as a function of pericentric distance; for $d_{\rm peri} \geq 50$ kpc, we assume no subhalo destruction (i.e. $N_{\rm HYDRO}/N_{\rm DMO} = 1$). Within the ELVIS halo catalogues, we then randomly destroy subhaloes as a function of their pericentric distance, given this probability of survival. In total, this removes approximately 25 per cent of the subhalo population at the selected mass scale ($M_{\rm peak} = 10^{7.9-9.75}\,\mathrm{M}_\odot$). Throughout the remainder of this work, we refer to these modified halo populations as comprising the 'Fat' ELVIS halo catalogues, given their inclusion of the destructive effects produced by the host's additional baryonic mass component. As hosts of the Milky Way's UFD population, we select subhaloes from our Fat ELVIS catalogues at $z = 0$ within the host virial radius and within a mass range of $M_{\rm peak} = 10^{7.9-9.75}\,\mathrm{M}_\odot$, following the stellar mass–halo mass (SMHM) relation of Garrison-Kimmel et al. (2014). This yields a population of 15, 269 subhaloes across the 48 ELVIS host systems.

The ELVIS merger trees include 75 snapshots ranging from $z = 125$ to $z = 0$. Following Fillingham et al. (2015), all halo properties are spline interpolated across the snapshots at a time resolution of 20 Myr, which enables more precise measurement of subhalo infall times and pericentric distances. To constrain the infall time ($t_{\rm infall}$) for each subhalo in our Fat ELVIS catalogues, we measure the redshift at which a subhalo was first and last accreted on to its host halo. In 51 per cent of cases, the first infall is the only infall, such that $t_{\rm first} = t_{\rm last}$. To account for the potential role of pre-processing, we also track the first infall on to any host halo with $M_{\rm peak} \geq 10^{10.8}\,\mathrm{M}_\odot$ at $z = 0$. Following the SMHM relation of Garrison-Kimmel et al. (2014), this host selection corresponds to systems that are similar to the Small Magellanic Cloud (SMC) or more massive. In total, roughly 65 per cent of subhaloes in our chosen mass range ($M_{\rm peak} = 10^{7.9-9.75}\,\mathrm{M}_\odot$) experience pre-processing, such that they are influenced by environment roughly 2.4 Gyr earlier on average (see also Wetzel, Deason & Garrison-Kimmel 2015a). Throughout this work, we take the last infall on to the current host (i.e. on to a Milky Way-like host) as the infall time for a subhalo, unless otherwise stated. In general, our primary results are qualitatively independent of the adopted definition of infall time.

As shown in Fig. 2, the distribution of subhalo infall times is very weakly dependent upon subhalo mass at $M_{\rm peak} < 10^{10}\,\mathrm{M}_\odot$, such that our results are largely independent of the assumed SMHM relation. Likewise, we find very little difference in the distribution of infall times for subhaloes associated with the Local Group-like, paired hosts versus the isolated hosts in the ELVIS suite, with subhaloes typically accreted <0.5 Gyr earlier in the Local Group-like simulations. In contrast, the typical infall time of a subhalo depends much more significantly on host-centric distance, with those systems located near the host biased towards early accretion. For our sample of low-mass haloes, the inclusion of tidal effects shifts the distribution of subhalo infall times by ∼0.7 Gyr earlier on average (see black dash–dotted line in Fig. 2). Our fiducial subhalo population, selected to have $0.15 < R/R_{\rm vir} < 0.5$ and $10^{8.4} < M_{\rm peak}/\mathrm{M}_\odot < 10^{9.2}$, includes a total of 1, 739 subhaloes and is well-matched to the UFD sample of Brown et al. (2014) based on host-centric distance and stellar mass, as shown relative to the greater MW UFD population in Fig. 1.

### 2.3 Methods

We employ a simple statistical method to quantify the probability that environmental mechanisms may be responsible for quenching star formation in a given population of subhaloes (i.e. UFDs). From the parent subhalo population, chosen to match a particular observed galaxy sample, we select (with replacement) a sample of $N$ random subhaloes. If all $N$ subhaloes are accreted on to their host halo (for the last time) at or before a given redshift, then for that redshift the entire set of subhaloes is considered quenched. This process is replicated across 10, 000 trials at each $z$, spanning from $z = 4$ to $z = 0$ at intervals of $\Delta z = 0.05$. The 'environmental quenching probability' as a function of cosmic time (or $z$) is then calculated

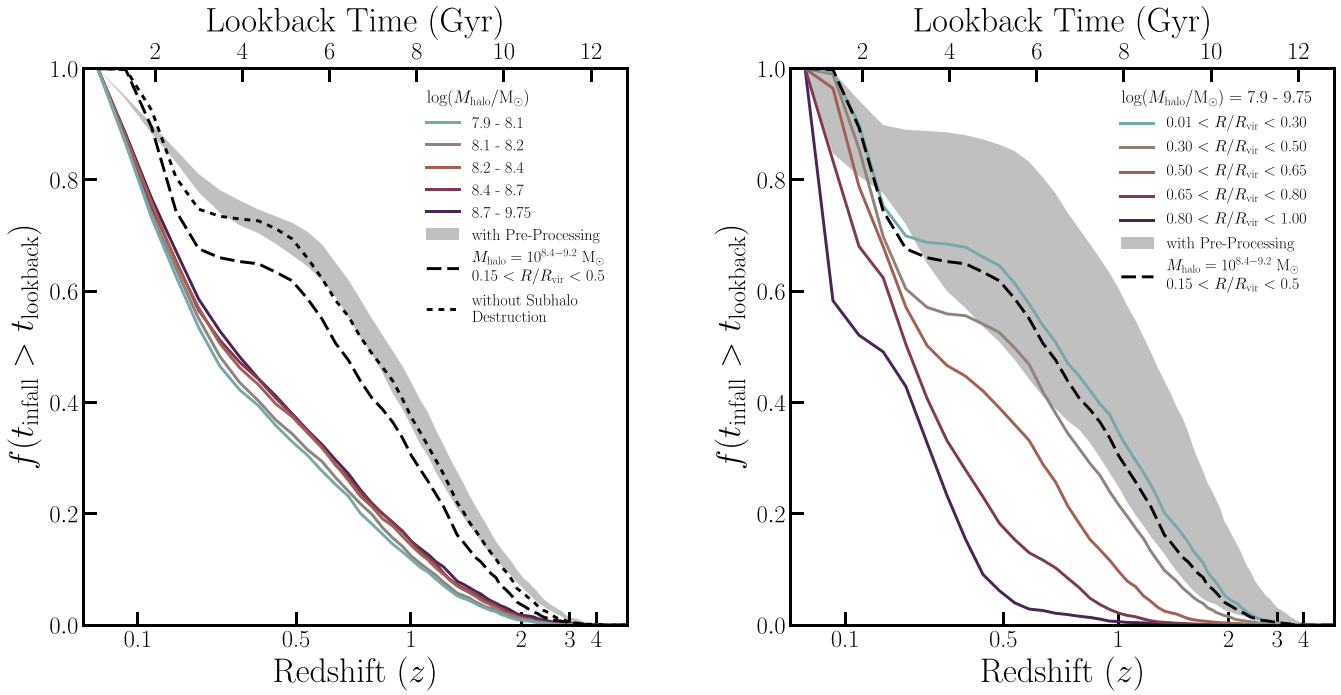


**Figure 2.** The cumulative distribution of infall times ($t_{\rm infall}$) as a function of redshift for subhaloes likely to host the Milky Way UFD satellite population. In both panels, the black long-dashed line corresponds to the distribution of infall times for our fiducial selection criteria, where subhaloes are restricted to $0.15 < R < 0.50\,R_{\rm vir}$ and $M_{\rm peak} = 10^{8.4-9.2}\,{\rm M}_\odot$. At *left*, we show the variation in infall times as a function of subhalo mass, for all subhaloes within $R_{\rm vir}$ at $z = 0$. At *right*, we plot the infall time distribution across bins in host-centric distance for all subhaloes with $M_{\rm peak} = 10^{7.9-9.75}\,{\rm M}_\odot$. Each bin in distance or mass contains an approximately equal number of subhaloes ($N \sim 3,050$). The dotted line illustrates the distribution of infall times for our fiducial sample without including the effects of subhalo disruption (i.e. using the original ELVIS catalogues versus the Fat ELVIS catalogues). Finally, the grey bands illustrate the corresponding distributions for infall on to a ≥SMC-like host halo prior to the last infall on to a Milky Way-like host halo (see Section 2.2). While the distribution of infall times is largely independent of subhalo mass (and thus our assumed SMHM relation), it is strongly dependent upon host-centric (i.e. galactocentric) distance.

as the ratio of trails where all $N$ systems quench relative to the total number of trials (i.e. 10, 000). Throughout the remainder of this work, we explore the dependence of this environmental quenching probability on the sample size ($N = 6$, 10, 20), the adopted infall time (e.g. allowing for pre-processing by lower mass hosts), and the fraction of the sample required to be quenched at a given redshift.

## 3 RESULTS

To determine if environmental effects were responsible for quenching the present-day lowest mass satellites of the Milky Way, we utilize our fiducial Fat ELVIS subhalo population to constrain the likelihood that all six galaxies in the Brown et al. (2014) UFD sample were accreted at early cosmic times – such that environmental quenching could reproduce the observed SFHs of these systems. From our fiducial subhalo sample, we randomly draw (with replacement) six subhaloes and evaluate – as a function of redshift – whether the entire sample of six was accreted by a given $z$. Repeating this exercise across 10, 000 trials, we compute the likelihood that a sample of six randomly chosen UFDs could be environmentally quenched as a function of cosmic time.

As shown in Fig. 3, there is a vanishingly small probability that six random subhaloes would all be accreted at high redshift (i.e. $z > 1$) or that the corresponding galaxies would be quenched by environmental process at such early cosmic time. At $z \sim 1$, after observations suggest that star formation halted in the UFD sample from Brown et al. (2014) including uncertainties of $\gtrsim$1 Gyr in the inferred SFHs, there is still an extremely low probability (< 0.1 per cent) that all six systems could be quenched via environmental effects. Allowing ∼1 Gyr for a satellite to quench following infall (Fillingham et al. 2015), such that all six UFDs must be accreted by $z \sim 1.3$ to quench by $z \sim 1$, only further decreases the potential impact of environmental quenching (see Fig. 3). While allowing for pre-processing in hosts down to SMC-like scales increases the possible effectiveness of environmental effects (see dashed plum line in Fig. 3), the likelihood that environment quenched the UFDs in the Brown et al. (2014) sample is remarkably low (< 1 per cent for $z_{\rm quench} > 2$). Overall, environmental mechanisms are unlikely to be responsible for the universally old stellar populations inferred for the Brown et al. (2014) UFD sample.

Including both Brown et al. (2014) and Weisz et al. (2014b), there are published SFHs for 10 UFDs, all indicating that star formation halted by $z \gtrsim 2$. Moreover, spectroscopic and/or photometric observations of (at least) a further 10 systems point to old (or metal-poor) stellar populations (e.g. Drlica-Wagner et al. 2015; Laevens et al. 2015a; Simon et al. 2015, 2017; Li et al. 2018; Torrealba et al. 2018). While these additional UFDs span a broader range of Galactocentric distance, with some potentially pre-processed by the Magellanic Clouds (Koposov et al. 2015; Bechtol et al. 2015; Drlica-Wagner et al. 2015; Yozin & Bekki 2015; Jethwa, Erkal & Belokurov 2016; Sales et al. 2017), the total sample of 20 UFDs creates a powerful data set with which to examine the role of environment. As expected, if we expand the sample of UFDs to all of those with well-measured SFHs ($N = 10$) or yet larger to $N = 20$, it

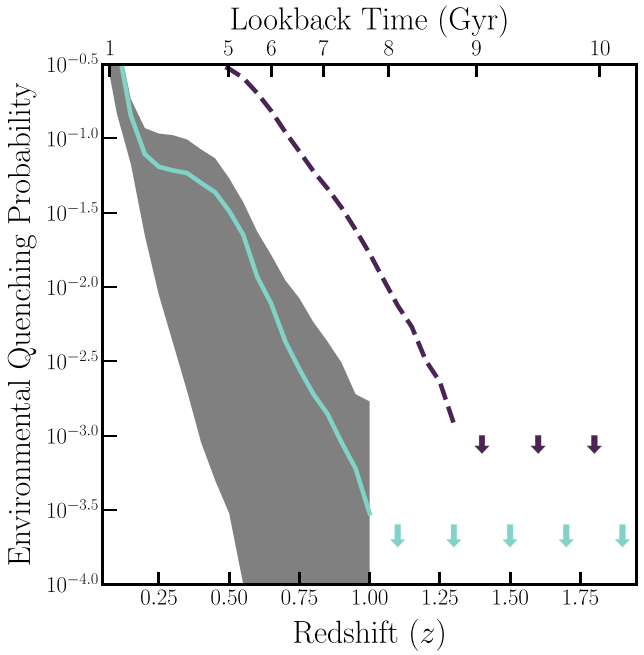


**Figure 3.** The probability that a random sample of six subhaloes, selected as likely UFD hosts, were all accreted prior to a given redshift ($z$). The aqua line illustrates this 'environmental quenching probability' as a function of redshift for our fiducial subhalo sample, while the grey shaded region illustrates the scatter associated with varying our selection of subhaloes across the range $0.01 < R/R_{\rm vir} < 0.9$. The dashed plum line includes the role of pre-processing (infall on to a ≥SMC-like host halo). The likelihood that environmental processes quenched the six UFDs from Brown et al. (2014) is relatively small (< 1 per cent).

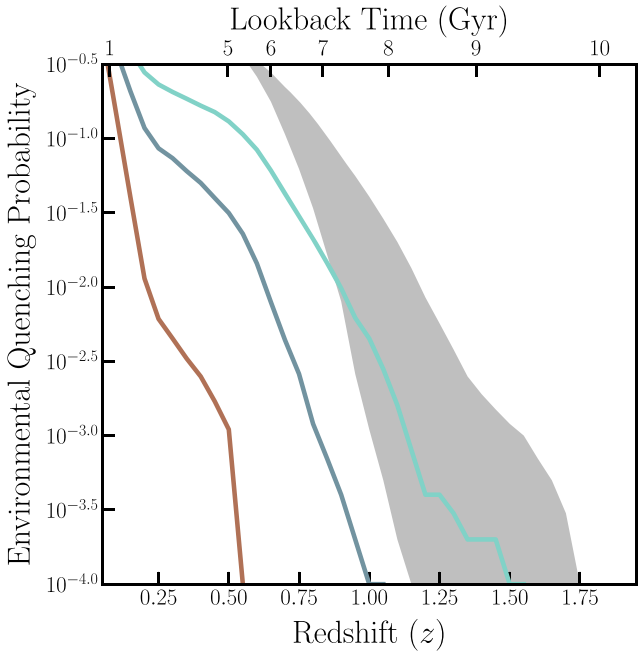


**Figure 4.** The probability that all (*solid lines*) or 75 per cent (*shaded region*) of a random sample of $N$ subhaloes, selected as likely UFD hosts, were accreted prior to a given redshift. For a parent subhalo population with $0.01 < R/R_{\rm vir} < 0.9$ and $10^{7.9} < M_{\rm peak}/{\rm M}_\odot < 10^{9.75}$, the aqua, sage, and sienna lines illustrate the environmental quenching probability as a function of redshift for subsamples of $N = 6$, 10, 20, representing our fiducial sample, the set of UFDs with SFHs, and the set of all UFDs with an estimated age, respectively. The grey shaded region illustrates the environmental quenching probability for samples of $N = 6$ to $N = 20$ UFDs, requiring that only 75 per cent of the population was accreted by the given redshift.

is even more difficult to explain the universally ancient stellar populations observed in terms of an environmental effect. Fig. 4 shows the probability that a sample of $N = 10$ (sage line) or $N = 20$ (sienna line) UFD satellites were quenched following infall on to the Milky Way halo as a function of cosmic time. We find that there is a $\lesssim$0.01 per cent probability that samples of this size were entirely accreted by $z = 2$. Even if we allow for late-time star formation in 25 per cent of the UFD population (see grey shaded region in Fig. 4), we find that environmental processes are unlikely to have been the dominant quenching mechanism for the current sample of known UFDs orbiting the Milky Way.

## 4 DISCUSSION

### 4.1 Quenching on the smallest scales

Our analysis shows that the old stellar populations (and lack of significant star formation at $z \lesssim 2$) observed in the Milky Way's UFD satellites are unlikely to be reproduced via environmental quenching. Instead, the observed SFHs of local UFDs are much more likely to have been truncated via reionization. Building upon the analysis of Fillingham et al. (2015, 2016), Fig. 5 presents a complete picture of the dominant physical processes driving late-time satellite quenching across more than seven orders of magnitude in satellite stellar mass. In particular, we plot the current constraints on the satellite quenching time-scale (measured relative to infall) as a function of satellite stellar mass; we caution that these measurements span a broad range of host halo masses (from $\sim 10^{12-15}$ M$_\odot$), but do describe a coherent physical scenario (Wetzel et al. 2013; Wheeler et al. 2014; Fillingham et al. 2015, 2016, 2018, see also De Lucia et al. 2012; Hirschmann et al. 2014; Davies et al. 2016).

As illustrated in Fig. 5, above a host-dependent critical mass scale, satellites are able to largely resist stripping forces, such that they are quenched on longer time-scales consistent with starvation (Larson, Tinsley & Caldwell 1980; Fillingham et al. 2015). Below this critical mass scale, which is roughly $M_\star \sim 10^8$ M$_\odot$ for Local Group-like hosts (Wheeler et al. 2014; Phillips et al. 2015), stripping is able to remove the fuel supply for star formation from infalling satellites, such that quenching occurs on roughly a dynamical time (Fillingham et al. 2015, 2016; Wetzel, Tollerud & Weisz 2015b). This critical mass scale increases with host halo mass, such that stripping is efficient at greater satellite masses in more massive host haloes (e.g. Kenney & Young 1989; Solanes et al. 2001; Boselli et al. 2014); meanwhile, there likely exists some limiting host mass (e.g. $M_{\rm halo} \sim 10^{11}$ M$_\odot$) for which stripping is inefficient on all mass scales and local environment is unable to quench satellites ($\tau_{\rm quench} \sim \tau_{\rm depl} > t_{\rm hubble}$). Finally, at the very lowest masses ($M_\star \lesssim 10^5$ M$_\odot$), reionization acts to suppress star formation, independent of environment (i.e. for both isolated and satellite systems). We illustrate this regime in Fig. 5 as the aqua shaded region.

Our results are consistent with recent hydrodynamical simulations of galaxy formation, which find that suppression of star formation by reionization is commonplace below a mass scale of $M_\star \lesssim 10^5$ M$_\odot$ (Benítez-Llambay et al. 2015; Fitts et al. 2017; Jeon, Besla & Bromm 2017; Aubert et al. 2018; Dawoodbhoy et al. 2018). While reionization halts the infall of new gas in low-mass haloes,

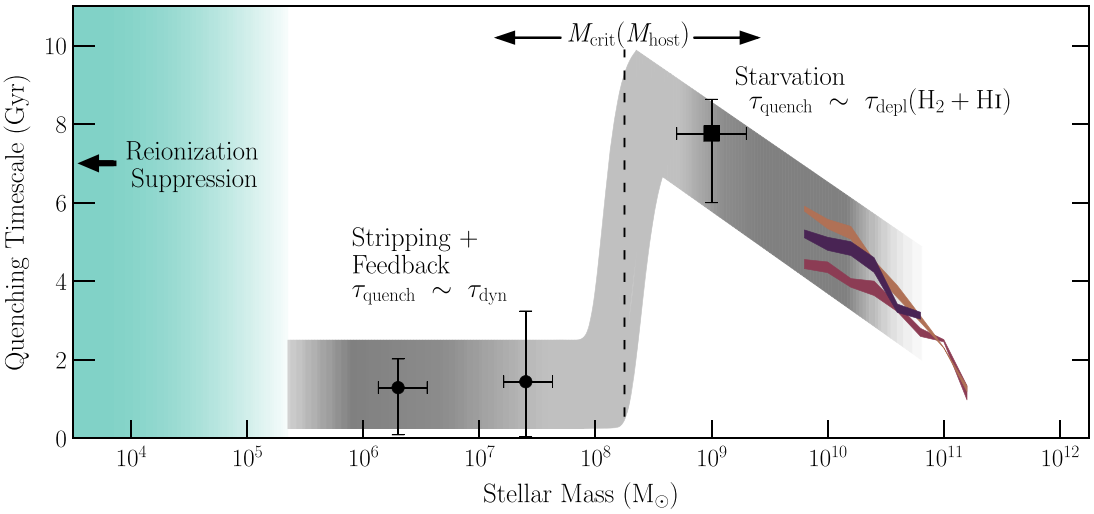


**Figure 5.** The dependence of the satellite quenching time-scale on satellite stellar mass in massive host haloes ($\gtrsim 10^{12}$ M$_\odot$), as adapted from Fillingham et al. (2015, 2016). The plum, sienna, and burgundy coloured bands show the constraints from Wetzel et al. (2013) for satellites in host haloes of $M_{\rm host} \sim 10^{12-13}$ M$_\odot$, $10^{13-14}$ M$_\odot$, and $10^{14-15}$ M$_\odot$, respectively. The black square and circles correspond to the typical quenching time-scale for intermediate- and low-mass satellites from Wheeler et al. (2014) and Fillingham et al. (2015), respectively. The light grey shaded regions highlight the expected dominant quenching mechanism as a function of satellite mass, while the vertical dashed black line denotes the critical mass scale below which satellite quenching becomes increasingly efficient for a roughly Milky Way-like host. This critical mass, at which the dominant quenching mechanism changes, should increase with host halo mass. Finally, the aqua shaded region highlights the mass range, where reionization is the most probable quenching mechanism.

residual star formation can be fuelled by the galaxy's existing gas reservoir so as to produce SFHs similar to those observed for UFDs (Oñorbe et al. 2015; Wheeler et al. 2015). Additionally, reignition of star formation after initial suppression via reionization may produce short and late periods of star formation (Ledinauskas & Zubovas 2018; Wright et al. 2019), such as that observed in Carina by Weisz et al. (2014b). Observations in the Local Volume also broadly suggest that the mass scale at which quenching via reionization dominates is approximately $M_\star \sim 10^5$ M$_\odot$ (e.g. Tollerud & Peek 2018). In particular, Leo T has a stellar mass of $M_\star \sim 10^{5.5}$ M$_\odot$, with a significant neutral gas reservoir (Ryan-Weber et al. 2008; Adams & Oosterloo 2018) and a complex SFH, including significant activity at $z < 1$ (de Jong et al. 2008; Clementini et al. 2012; Weisz et al. 2012). At a distance of $> 400$ kpc from the Milky Way (Irwin et al. 2007), Leo T likely represents the tail of the star-forming field population, having a dark matter halo mass greater than that at which reionization suppresses gas cooling. Studies of stellar and gas kinematics in Leo T suggest a halo mass of $\sim 10^9$ M$_\odot$ (Simon & Geha 2007; Ryan-Weber et al. 2008). And XVI (Ibata et al. 2007), a satellite of M31 with a stellar mass of $\gtrsim 10^5$ M$_\odot$ and an SFH that extends to $z \sim 0.5$ (Weisz et al. 2014a; Monelli et al. 2016), was potentially a similar system prior to being accreted by M31 and quenched via environmental mechanisms. While Leo T and And XVI support a mass scale for quenching via reionization of $M_\star \sim 10^5$ M$_\odot$ ($M_{\rm halo} \sim 10^9$ M$_\odot$), recent observations of additional low-mass satellites of M31 indicate that the relevant mass scale may be yet lower ($M_\star \sim 10^{4.5}$ M$_\odot$, Martin et al. 2016b, 2017). It is important to note that there is likely not a clearly defined stellar mass scale at which reionization is effective, given the potentially large scatter in the SMHM relation at low masses (Garrison-Kimmel et al. 2017a).

Taking $M_\star \sim 10^5$ M$_\odot$ ($M_{\rm halo} \sim 10^9$ M$_\odot$) as the scale at which reionization suppresses star formation across all environments, we predict a population of $\gtrsim 250$ UFDs within $1 < R/R_{\rm vir} < 2$ of the Milky Way and M31, based on counts of haloes with $M_{\rm halo} = 10^{7.9-9.75}$ M$_\odot$ in the Fat ELVIS catalogues across all 36 simulations.[2] All of these systems are expected to be dominated by ancient stellar populations. While some will have interacted with the Milky Way and/or M31, a relatively large fraction ($> 50$ per cent) of haloes at these distances are true 'field' systems, having never spent time as a subhalo. Future imaging surveys, such as the Large Synoptic Survey Telescope (Ivezic et al. 2008), are expected to discover much of this population in the coming decade, opening new avenues to study the suppression of star formation on the smallest scales. The total number of field UFDs will not only depend on the mass scale at which reionization suppresses ongoing star formation at high $z$, but also the yet lower scale at which it is able to suppress all star formation (e.g. Bullock, Kravtsov & Weinberg 2000; Somerville 2002).

### 4.2 The curious case of Eri II

If reionization truly quenches all low-mass galaxies, independent of environment, we would expect that isolated UFDs should host ancient stellar populations similar to those observed for known UFD satellites. The recent discovery of Eridanus II at a distance of $\gtrsim 350$ kpc from the Milky Way (Bechtol et al. 2015; Li et al. 2017) has offered the opportunity to probe the SFH of a 'field' UFD in significant detail. However, at a Galactocentric distance of $\sim 1.2 R_{\rm vir}$, Eri II cannot be considered an isolated system, unaffected by potential environmental effects. A significant fraction of systems at such distances are associated with 'backsplash' haloes (Teyssier, Johnston & Kuhlen 2012; Garrison-Kimmel et al. 2014; Fillingham et al. 2018), which previously passed within the host's (i.e. Milky Way's) virial radius before returning to the field.

[2]On average, the 12 paired host simulations have slightly more haloes in the $1 < R/R_{\rm vir} < 2$ range and a smaller fraction of these being backsplash haloes.

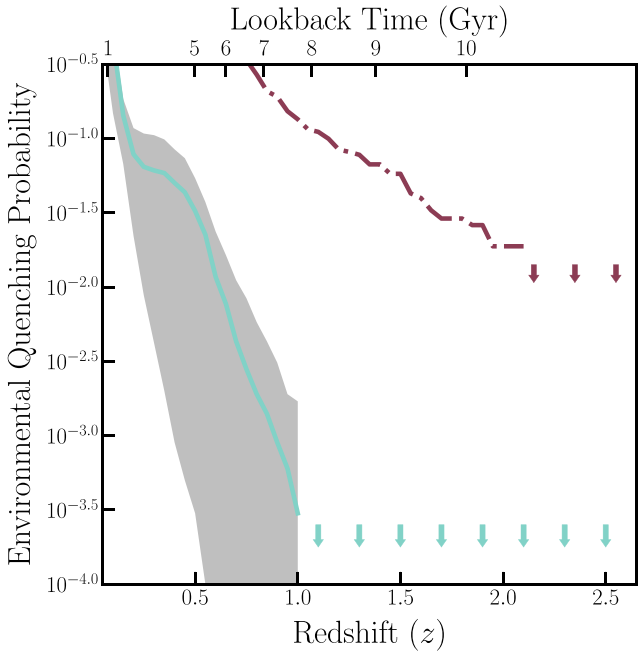


**Figure 6.** The probability that a randomly selected Eri II-like halo was accreted by the Milky Way as a function of cosmic time (burgundy dash–dotted line). For comparison, we overplot the probability that a sample of six subhaloes were accreted by the same redshift (from Fig. 3). While Eri II is unlikely to have been quenched by environment, the ancient stellar populations observed in current samples of UFD satellites argue more strongly against environment's role in suppressing star formation on the smallest scales.

While recent observations show no signs of late-time star formation (Li et al. 2017, but see also Koposov et al. 2015; Crnojević et al. 2016), Eri II – as a solitary system with an unknown orbital history – places limited constraints on the dominant mechanism responsible for suppressing star formation on the smallest scales. As shown in Fig. 6, the current sample of Milky Way UFD satellites already places a stronger constraint on the role of environment. To test whether Eri II is likely to have been quenched by environment, we select subhaloes from our Fat ELVIS catalogues, matching the mass ($8.9 < M_{\rm peak}/{\rm M}_{\odot} < 9.75$), host-centric line-of-sight velocity ($-90\,{\rm km\,s^{-1}} < V_{\ell{\rm os}} < -40\,{\rm km\,s^{-1}}$), and host-centric distance ($0.9 < R/R_{\rm vir} < 1.9$) of Eri II (Li et al. 2017).[3] From the resulting sample of 274 subhaloes, we compute the infall distribution as a function of cosmic time (see Fig. 6), which corresponds to the likelihood that environment played a role in quenching star formation in Eri II. We find that there is a ∼10 per cent chance that Eri II was quenched via an interaction with the Milky Way at $z \sim 1$. While Eri II is unlikely to have been quenched due to an interaction with the Milky Way at $z > 2$ (so as to produce a purely old stellar population), the measured SFHs for the existing sample of UFD satellites orbiting the Milky Way already argue more strongly against environment's role in suppressing star formation on the smallest scales.

[3]The adopted phase-space range was selected to encompass velocity and distance errors, as well as a possibly higher than originally assumed total velocity, following suit based on recently derived velocities for UFDs from *Gaia* Data Release 2 (Fritz et al. 2018b; Simon 2018).

## 5 SUMMARY

Using the ELVIS suite of Milky Way- and Local Group-like *N*-body simulations to constrain the infall times for subhaloes likely to host the ultra-faint satellite population of the Milky Way, we explore the potential role of environment in suppressing star formation on small scales. Our principal results are as follows:

(i) When incorporating the effects of subhalo tidal disruption due to the inclusion of the host's baryonic component, we find a shift in the typical infall time of ∼0.7 Gyr for subhaloes in the mass range of $M_{\rm halo} = 10^{7.9-9.75}\,{\rm M}_{\odot}$, such that subhaloes are preferentially accreted at later cosmic time versus the same subhaloes in a pure dark matter-only, *N*-body simulation.

(ii) For the six UFDs included in the Brown et al. (2014) sample, we find that there is a $\lesssim$0.1 per cent probability that the Milky Way environment was solely responsible for quenching their star formation at $z > 1$.

(iii) For larger samples of UFDs, the likelihood that environment plays a dominant role in quenching decreases dramatically, such that there is a < 0.01 per cent probability that environmental mechanisms are responsible for quenching all 10 UFDs included in the Brown et al. (2014) and Weisz et al. (2014b) samples.

(iv) Given the inability of environmental effects to reproduce the observed SFHs of observed UFDs, we conclude that reionization is the most likely mechanism by which star formation is suppressed on the smallest scales.

(v) Finally, we predict that there is a population of $\gtrsim$ 250 UFDs within $1 < R/R_{\rm vir} < 2$ of the Milky Way and M31, all with ancient stellar populations. Future imaging surveys, such as LSST, will be able to uncover much of this population.

Combined with results from Fillingham et al. (2015, 2016), our results produce a coherent physical picture describing the dominant quenching mechanism across the entire range of satellite (and host) masses (see Fig. 5). At the very smallest scales, we argue that the suppression of star formation is largely independent of environment and set by the minimum halo mass at which reionization curtails gas accretion.

## ACKNOWLEDGEMENTS

We thank Tyler Kelley, Dan Weisz, Josh Simon, Alex Riley, and Mary Jenkins for helpful discussions regarding this project. This work was supported in part by NSF grants AST-1518257, AST-1518291, AST-1517226, and AST-1815475. MBK also acknowledges support from NSF CAREER grant AST-1752913 and NASA grant NNX17AG29G. Additional support for this work was provided by NASA through grants GO-12914, AR-13888, AR-13896, GO-14191, AR-14282, AR-14289, AR-14554, and AR-15006 from the Space Telescope Science Institute, which is operated by the Association of Universities for Research in Astronomy, Inc., under NASA contract NAS 5-26555. MKRW acknowledges support from the National Science Foundation Graduate Research Fellowship. This material is based upon work supported by the National Science Foundation Graduate Research Fellowship Program under Grant No. DGE-1321846.

This research made use of `astropy`, a community-developed core PYTHON package for Astronomy (Astropy Collaboration et al. 2013). Additionally, the PYTHON packages `numpy` (Walt, Colbert & Varoquaux 2011), `ipython` (Pérez & Granger 2007), `scipy` (Jones et al. 2001), and `matplotlib` (Hunter 2007) were utilized for the majority of our data analysis and presentation.

## REFERENCES


Adams E. A. K., Oosterloo T. A., 2018, A&A, 612, A26
Astropy Collaboration et al., 2013, A&A, 558, A33
Aubert D. et al., 2018, ApJ, 856, L22
Bechtol K. et al., 2015, ApJ, 807, 50
Belokurov V. et al., 2007, ApJ, 654, 897
Belokurov V. et al., 2010, ApJ, 712, L103
Benítez-Llambay A., Navarro J. F., Abadi M. G., Gottlöber S., Yepes G., Hoffman Y., Steinmetz M., 2015, MNRAS, 450, 4207
Bettinelli M., Hidalgo S. L., Cassisi S., Aparicio A., Piotto G., 2018, MNRAS, 476, 71
Boselli A., Cortese L., Boquien M., Boissier S., Catinella B., Gavazzi G., Lagos C., Saintonge A., 2014, A&A, 564, A67
Boylan-Kolchin M., Weisz D. R., Bullock J. S., Cooper M. C., 2016, MNRAS, 462, L51
Brooks A. M., Zolotov A., 2014, ApJ, 786, 87
Brooks A. M., Kuhlen M., Zolotov A., Hooper D., 2013, ApJ, 765, 22
Brown T. M. et al., 2012, ApJ, 753, L21
Brown T. M. et al., 2014, ApJ, 796, 91
Bullock J. S., Kravtsov A. V., Weinberg D. H., 2000, ApJ, 539, 517
Caldwell N. et al., 2017, ApJ, 839, 20
Clementini G., Cignoni M., Contreras Ramos R., Federici L., Ripepi V., Marconi M., Tosi M., Musella I., 2012, ApJ, 756, 108
Crnojević D., Sand D. J., Zaritsky D., Spekkens K., Willman B., Hargis J. R., 2016, ApJ, 824, L14
D'Onghia E., Springel V., Hernquist L., Keres D., 2010, ApJ, 709, 1138
Davies L. J. M. et al., 2016, MNRAS, 455, 4013
Dawoodbhoy T. et al., 2018, MNRAS, 480, 1740
de Jong J. T. A. et al., 2008, ApJ, 680, 1112
De Lucia G., Weinmann S., Poggianti B. M., Aragón-Salamanca A., Zaritsky D., 2012, MNRAS, 423, 1277
Drlica-Wagner A. et al., 2015, ApJ, 813, 109
Efstathiou G., 1992, MNRAS, 256, 43P
Fillingham S. P., Cooper M. C., Wheeler C., Garrison-Kimmel S., Boylan-Kolchin M., Bullock J. S., 2015, MNRAS, 454, 2039
Fillingham S. P., Cooper M. C., Pace A. B., Boylan-Kolchin M., Bullock J. S., Garrison-Kimmel S., Wheeler C., 2016, MNRAS, 463, 1916
Fillingham S. P., Cooper M. C., Boylan-Kolchin M., Bullock J. S., Garrison-Kimmel S., Wheeler C., 2018, MNRAS, 477, 4491
Fitts A. et al., 2017, MNRAS, 471, 3547
Frebel A., Simon J. D., Kirby E. N., 2014, ApJ, 786, 74
Fritz T. K., Lokken M., Kallivayalil N., Wetzel A., Linden S. T., Zivick P., Tollerud E. J., 2018a, ApJ, 860, 164
Fritz T. K., Battaglia G., Pawlowski M. S., Kallivayalil N., van der Marel R., Sohn T. S., Brook C., Besla G., 2018b, A&A, 619, A103
Garrison-Kimmel S. et al., 2017b, MNRAS, 471, 1709
Garrison-Kimmel S., Boylan-Kolchin M., Bullock J. S., Lee K., 2014, MNRAS, 438, 2578
Garrison-Kimmel S., Bullock J. S., Boylan-Kolchin M., Bardwell E., 2017a, MNRAS, 464, 3108
Hirschmann M., De Lucia G., Wilman D., Weinmann S., Iovino A., Cucciati O., Zibetti S., Villalobos Á., 2014, MNRAS, 444, 2938
Hunter J. D., 2007, Comput. Sci. Eng., 9, 90
Ibata R., Martin N. F., Irwin M., Chapman S., Ferguson A. M. N., Lewis G. F., McConnachie A. W., 2007, ApJ, 671, 1591
Irwin M. J. et al., 2007, ApJ, 656, L13
Ivezić Z. et al., 2008, preprint (arXiv:0805.2366)
Jeon M., Besla G., Bromm V., 2017, ApJ, 848, 85
Jethwa P., Erkal D., Belokurov V., 2016, MNRAS, 461, 2212
Jones E., Oliphant T., Peterson P. et al., 2001, SciPy: Open Source Scientific Tools for Python, Available at: http://www.scipy.org/
Kelley T., Bullock J. S., Garrison-Kimmel S., Boylan-Kolchin M., Pawlowski M. S., Graus A. S., 2018, preprint (arXiv:1811.12413)
Kenney J. D. P., Young J. S., 1989, ApJ, 344, 171
Kirby E. N., Boylan-Kolchin M., Cohen J. G., Geha M., Bullock J. S., Kaplinghat M., 2013, ApJ, 770, 16
Kirby E. N., Simon J. D., Cohen J. G., 2015a, ApJ, 810, 56
Kirby E. N., Cohen J. G., Simon J. D., Guhathakurta P., 2015b, ApJ, 814, L7
Kirby E. N., Cohen J. G., Simon J. D., Guhathakurta P., Thygesen A. O., Duggan G. E., 2017, ApJ, 838, 83
Komatsu E. et al., 2011, ApJS, 192, 18
Koposov S. E. et al., 2018, MNRAS, 479, 5343
Koposov S. E., Belokurov V., Torrealba G., Evans N. W., 2015, ApJ, 805, 130
Laevens B. P. M. et al., 2015a, ApJ, 802, L18
Laevens B. P. M. et al., 2015b, ApJ, 813, 44
Larson D. et al., 2011, ApJS, 192, 16
Larson R. B., Tinsley B. M., Caldwell C. N., 1980, ApJ, 237, 692
Ledinauskas E., Zubovas K., 2018, A&A, 615, A64
Li T. S. et al., 2017, ApJ, 838, 8
Li T. S. et al., 2018, ApJ, 857, 145
Martin N. F. et al., 2009, ApJ, 705, 758
Martin N. F. et al., 2015, ApJ, 804, L5
Martin N. F. et al., 2016a, MNRAS, 458, L59
Martin N. F. et al., 2016b, ApJ, 833, 167
Martin N. F. et al., 2017, ApJ, 850, 16
McConnachie A. W., 2012, AJ, 144, 4
Monelli M. et al., 2016, ApJ, 819, 147
Okamoto S., Arimoto N., Yamada Y., Onodera M., 2008, A&A, 487, 103
Okamoto S., Arimoto N., Yamada Y., Onodera M., 2012, ApJ, 744, 96
Oman K. A., Hudson M. J., Behroozi P. S., 2013, MNRAS, 431, 2307
Oñorbe J., Boylan-Kolchin M., Bullock J. S., Hopkins P. F., Kereš D., Faucher-Giguère C.-A., Quataert E., Murray N., 2015, MNRAS, 454, 2092
Pérez F., Granger B. E., 2007, Comput. Sci. Eng., 9, 21
Phillips J. I., Wheeler C., Cooper M. C., Boylan-Kolchin M., Bullock J. S., Tollerud E., 2015, MNRAS, 447, 698
Quinn T., Katz N., Efstathiou G., 1996, MNRAS, 278, L49
Rocha M., Peter A. H. G., Bullock J., 2012, MNRAS, 425, 231
Ryan-Weber E. V., Begum A., Oosterloo T., Pal S., Irwin M. J., Belokurov V., Evans N. W., Zucker D. B., 2008, MNRAS, 384, 535
Sales L. V., Navarro J. F., Kallivayalil N., Frenk C. S., 2017, MNRAS, 465, 1879
Sand D. J., Olszewski E. W., Willman B., Zaritsky D., Seth A., Harris J., Piatek S., Saha A., 2009, ApJ, 704, 898
Sand D. J., Seth A., Olszewski E. W., Willman B., Zaritsky D., Kallivayalil N., 2010, ApJ, 718, 530
Sand D. J., Strader J., Willman B., Zaritsky D., McLeod B., Caldwell N., Seth A., Olszewski E., 2012, ApJ, 756, 79
Sawala T., Pihajoki P., Johansson P. H., Frenk C. S., Navarro J. F., Oman K. A., White S. D. M., 2017, MNRAS, 467, 4383
Simon J. D. et al., 2015, ApJ, 808, 95
Simon J. D. et al., 2017, ApJ, 838, 11
Simon J. D., 2018, ApJ, 863, 89
Simon J. D., Geha M., 2007, ApJ, 670, 313
Skillman E. D. et al., 2017, ApJ, 837, 102
Solanes J. M., Manrique A., García-Gómez C., González-Casado G., Giovanelli R., Haynes M. P., 2001, ApJ, 548, 97
Somerville R. S., 2002, ApJ, 572, L23
Teyssier M., Johnston K. V., Kuhlen M., 2012, MNRAS, 426, 1808
Thoul A. A., Weinberg D. H., 1996, ApJ, 465, 608
Tollerud E. J., Peek J. E. G., 2018, ApJ, 857, 45
Torrealba G. et al., 2016, MNRAS, 463, 712
Torrealba G. et al., 2018, MNRAS, 475, 5085
Walker M. G. et al., 2016, ApJ, 819, 53
Walt S. v. d., Colbert S. C., Varoquaux G., 2011, Comput. Sci. Eng., 13, 22
Webster D., Frebel A., Bland-Hawthorn J., 2016, ApJ, 818, 80
Weisz D. R. et al., 2012, ApJ, 748, 88
Weisz D. R. et al., 2014a, ApJ, 789, 24
Weisz D. R., Dolphin A. E., Skillman E. D., Holtzman J., Gilbert K. M., Dalcanton J. J., Williams B. F., 2014b, ApJ, 789, 147
Weisz D. R., Dolphin A. E., Skillman E. D., Holtzman J., Gilbert K. M., Dalcanton J. J., Williams B. F., 2015, ApJ, 804, 136

Wetzel A. R., Tinker J. L., Conroy C., van den Bosch F. C., 2013, MNRAS, 432, 336
Wetzel A. R., Deason A. J., Garrison-Kimmel S., 2015a, ApJ, 807, 49
Wetzel A. R., Tollerud E. J., Weisz D. R., 2015b, ApJ, 808, L27
Wheeler C., Phillips J. I., Cooper M. C., Boylan-Kolchin M., Bullock J. S., 2014, MNRAS, 442, 1396
Wheeler C., Oñorbe J., Bullock J. S., Boylan-Kolchin M., Elbert O. D., Garrison-Kimmel S., Hopkins P. F., Kereš D., 2015, MNRAS, 453, 1305
Willman B. et al., 2005a, AJ, 129, 2692
Willman B. et al., 2005b, ApJ, 626, L85
Wright A. C., Brooks A. M., Weisz D. R., Christensen C. R., 2019, MNRAS, 482, 1176
York D. G. et al., 2000, AJ, 120, 1579
Yozin C., Bekki K., 2015, MNRAS, 453, 2302
Zucker D. B. et al., 2006a, ApJ, 643, L103
Zucker D. B. et al., 2006b, ApJ, 650, L41

This paper has been typeset from a TEX/LATEX file prepared by the author.